



Universiteit
Leiden
The Netherlands

Neural processing of goal and non-goal directed movements on the smartphone

Kock, R.; Ceolini E.; Groenewegen, L.; Ghosh, A.

Citation

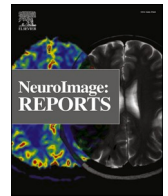
Kock, R., Groenewegen, L., & Ghosh, A. (2023). Neural processing of goal and non-goal directed movements on the smartphone. *Neuroimage: Reports*, 3(2).
doi:10.1016/j.ynirp.2023.100164

Version: Publisher's Version

License: [Creative Commons CC BY 4.0 license](#)

Downloaded from: <https://hdl.handle.net/1887/3590738>

Note: To cite this publication please use the final published version (if applicable).



Neural processing of goal and non-goal-directed movements on the smartphone

Ruchella Kock, Enea Ceolini, Lysanne Groenewegen, Arko Ghosh*

Cognitive Psychology Unit, Institute of Psychology, Leiden University, the Netherlands

ABSTRACT

The discrete behavioral events captured on the smartphone touchscreen may help unravel real-world neural processing. We find that neural signals (EEG) surrounding a touchscreen event show a distinctly contralateral motor preparation followed by visual processing, and the consolidation of information. We leveraged these events in conjunction with kinematic recordings of the thumb and an artificial neural network to separate highly similar movements according to whether they resulted in a smartphone touch (goal-directed) or not (non-goal-directed). Despite their kinematic similarity, the signatures of neural control of movement and the post-movement processing were substantially dampened for the non-goal-directed movements, and these movements uniquely evoked error-related signals. We speculate that these apparently unnecessary movements are common in the real world and although inconsequential the brain provides limited motor preparation and tracks the action outcome. The neural signals surrounding discrete smartphone events can enable the study of neural processes that are difficult to capture in conventional laboratory-based tasks.

1. Introduction

How the human brain generates real-world behavior is sparsely understood. This is partly because artificial behaviors – disconnected from daily life – dominate the study of neuro-behavioral correlates, and how to use what has been learned using such paradigms to understand the real-world behavioral outputs is not clear. Behaviors such as the reaction time task and the less instructed voluntary finger movements have been instrumental in isolating specific neural processes for the neural control of movement and sensory processing. Still, in the real world, multiple neural processes may be simultaneously engaged and the statistical properties of the tasks are fundamentally distinct from what is experienced in the real world (Ingram et al., 2008; Kayser et al., 2004). There is a fast emerging understanding of the complex naturalistic statistics of sounds, images, and movements, and this recent paradigm shift has already helped unravel specific neural processes tuned to naturalistic information and movements (Sonkusare et al., 2019; Ingram et al., 2011). Smartphones are ubiquitous in modern human behavior and they are a source of complex visual information largely driven by touchscreen interactions (including typing, scrolling, or any other gesture expressed via the screen). Studying the brain activity underlying this behavior is not only relevant to addressing the neural basis of a common behavior but may also help discover how a range of neural processes are orchestrated to generate behavior that is truly meaningful to daily life.

In this report, we shall first describe the neural signals surrounding

smartphone interactions. One of the main challenges here is to derive interpretable brain signals. The discrete nature of the smartphone interactions provide a decisive behavioral landmark. Therefore, we can simply time-lock the EEG signals to the touchscreen interaction events captured at a millisecond resolution (Balerna and Ghosh, 2018). This allows us to leverage the conventional event-related potential framework to recognize the underlying neural processes based on the well-studied signal features. For instance, bilateral negativity over the sensorimotor electrodes and desynchronization (diminished oscillatory power) of beta oscillations can help infer the underlying motor processes (Kilavik et al., 2013; Qing Cui and Deecke, 1999; Kristeva et al., 1990). Furthermore, negativity over the visual electrodes can indicate visual processing and the frontal-to-central wave of positivity can help reveal memory-related information consolidation (Kilavik et al., 2013; Picton, 1992; Houdayer et al., 2020; Shibasaki and Hallett, 2006; Leocani et al., 2001).

When gathering the neuro-behavioral data, we chanced upon the phenomena that when engaged on the smartphone there were a substantial number of thumb movements that produced no interactions at all. This was surprising to us, as according to a widely held notion (perhaps even implicit in experimental design), when engaged in behavior, movements generated are actively aligned to the behavioral goal by the pre-frontal cortex (Matsumoto and Tanaka, 2004). Moreover, as an example of the implicit assumption of goal-oriented movements in experimental design, in visual response time tasks the timing of

* Corresponding author. Leiden University, Wassenaarseweg 52, Leiden, 2333 AK, the Netherlands.

E-mail address: a.ghosh@fsw.leidenuniv.nl (A. Ghosh).

the finger movement in response to the visual stimuli is carefully measured whereas the rest of the inter-stimuli finger movements are simply neglected. However, a scattered set of observations challenge the notion by unraveling movements that are not simply related to the set behavioral goal. Firstly, according to subjective self-reports inconsequential movements dubbed *fidgiting* are ubiquitous in the real world (Mehrabian and Friedman, 1986). Secondly, in the laboratory, there is emerging evidence for the idea that the cortex is less engaged during the task-irrelevant (non-goal-directed) vs. the relevant (goal-directed) actions. According to invasive neural recordings from the frontal eye field of the monkey cortex, the beta-band remains synchronized (i.e., sustained oscillatory power) during the non-goal-directed saccades (Sendhilnathan et al., 2021). In humans, when instructed to aimlessly touch the screen, the beta desynchronization and the motor-related potentials are diminished compared to the goal-directed touches aimed at a certain location (Pereira et al., 2017). While these studies demonstrate the capacity to generate non-goal-directed actions, how they are generated when engaged in real-world behavior remains unclear.

The extent of the withdrawal of cortical engagement during non-goal-directed movements is also not clear. Is body-related (touch or proprioception) sensory processing also diminished during these movements? There is sparse evidence to suggest that the neural signals associated with task-irrelevant inputs from the body are diminished (Staines et al., 2000). For the hand, this form of sensory gating is visible in the mid-latency signals at about ~ 70 ms (Adams et al., 2017). However, these processes may be inter-mixed with the widespread movement-related sensory gating that is thought to suppress sensory information in anticipation of the barrage of inputs accompanying a movement (Rossini et al., 1999). This form of gating is visible in the early somatosensory signals at about ~ 50 ms and the signals at this latency may be diminished during the non-goal-directed movements.

Seeking to better understand the neural basis of the apparently non-goal-directed movements when on the smartphone, we analyzed the surrounding neural signals. Capturing the non-goal-directed neural signals is conceptually more complex than capturing the neural signals surrounding the smartphone touches. Even if they are captured, they may not be simply comparable to the neural signals time-locked to the smartphone interactions. For instance, the difference in the neural signals between smartphone touches and non-goal-directed movements could be attributed to the differences in the peripheral signal features chosen to time-lock the neural signals. Moreover, while a motion sensor attached to the thumb can detect movements with high fidelity, it cannot directly yield decisive temporal landmarks that could be used to study kinematically similar goal and non-goal-directed movements from a series of signal fluctuations – where one movement is followed by another. To circumvent these issues, we trained an artificial neural network to mark smartphone touchscreen interaction timings based on the movement sensor signals. We expected the model to correctly identify smartphone touches (true positives) and anticipated that the kinematically highly similar movements - if they exist - would yield false positives (i.e., movement without a touchscreen touch). As for both the goal and the non-goal-directed movements the temporal landmarks can be based on the same set of learned features, this approach offers an opportunity to contrast the time-locked neural signals. Finally, using artificial tactile stimulations interspersed through the observation we addressed somatosensory gating during the two movement types.

We reveal how neural processes are orchestrated surrounding smartphone behavior, by combining data-driven behavioral modeling, smartphone touchscreen interaction logs, and parametric statistics of event-related (spectral) analysis (across all electrodes and broad time range) surrounding the discrete events. Our analysis reveals a stark distinction between the goal and non-goal-directed actions spanning a range of neural processes.

2. Results

2.1. The neural signals surrounding smartphone touchscreen events

The event-related brain signals surrounding the smartphone touchscreen events spanned ~ 2.3 s. The initial signals starting at -700 ms consisted of a slow rise of signals (positivity) over the contralateral to the movement (i.e., left side) sensorimotor electrodes (Fig. 1, Supplementary Movie 1). This rise was followed by gradual negativity starting at about -300 ms in the same region. This negativity lasted till 200 ms, with the negativity shifting to the occipital electrodes where it was sustained for another 250 ms. This was followed by a frontal to central positivity spanning between 500 and 700 ms. These signals were followed by more topologically scattered activations that finally terminated by ~ 1.6 s. The initial sensorimotor activations were notably contralateral and in contrast to the initially bilateral sensorimotor activity described in laboratory-designed behaviors. Indeed, we could reproduce bilateral negativity when we instructed participants to touch a smartphone-like surface (Supplementary Movie 2).

Time-frequency analysis revealed strong beta-band desynchronization (reduced power) surrounding the touchscreen interactions. The desynchronization over the sensorimotor electrodes appeared ~ 1.2 s before the interaction and strengthened up to the interaction. The pre-interaction desynchronization appeared asymmetric with lower power over the contralateral electrodes. Strong event-related desynchronization persisted after the interaction and the oscillations rebounded by 550 ms over the central electrodes. The desynchronization was not limited to the beta-band during the interaction but extended to the alpha and gamma bands (Fig. 1, Supplementary Movie 3 for the beta-band, Supplementary Movie 4 for the alpha-band).

2.2. The identification of goal and non-goal-directed smartphone movements

We deployed an artificial neural network to find landmarks on the movement signals corresponding to the touchscreen interaction. The model performed with an F2 score (a measure of model recall and precision, with a higher weight on the recall) of 0.35 (median of all trained subjects, $N = 68$) and 0.34 (median based on subjects considered here, $N = 32$) (Supplementary Table 1, Supplementary Fig. 1). The identified landmarks which did coincide with the smartphone touch (within ± 100 ms) were categorized as goal-directed movements. The identified landmarks that did not coincide with a smartphone interaction – non-goal-directed movements – revealed a degree of kinematic similarity with the goal-directed movements (Fig. 2a' shows an example participant, see Supplementary Fig. 2 for all participants). As we were interested in studying the neural correlates contrasting these two movement types notwithstanding any kinematic differences, we further considered only those subjects ($N = 36$) with highly similar kinematic fluctuations between the two movement types ($R > 0.8$, See Supplementary Methods for the distribution of Pearson Rs).

Both the non-goal-directed movements and the goal-directed movements were common in the selected population (Supplementary Fig. 1b). The inter-event intervals were typically separated by ~ 1 s for the goal-directed movements whereas the non-goal-directed movements were separated by a broader distribution with a primary peak under ~ 1 s and a secondary peak at ~ 10 s (Supplementary Fig. 1c). The non-goal-directed movements were more likely to occur right after the goal-directed movement rather than before ($t = -2.6910$, $p = 0.0114$, paired t -test, Supplementary Fig. 1d).

2.3. EEG potentials surrounding goal-directed vs. non-goal-directed movements

The temporal landmarks deduced by the artificial neural network were used to time-lock the EEG signals for both goal and non-goal-

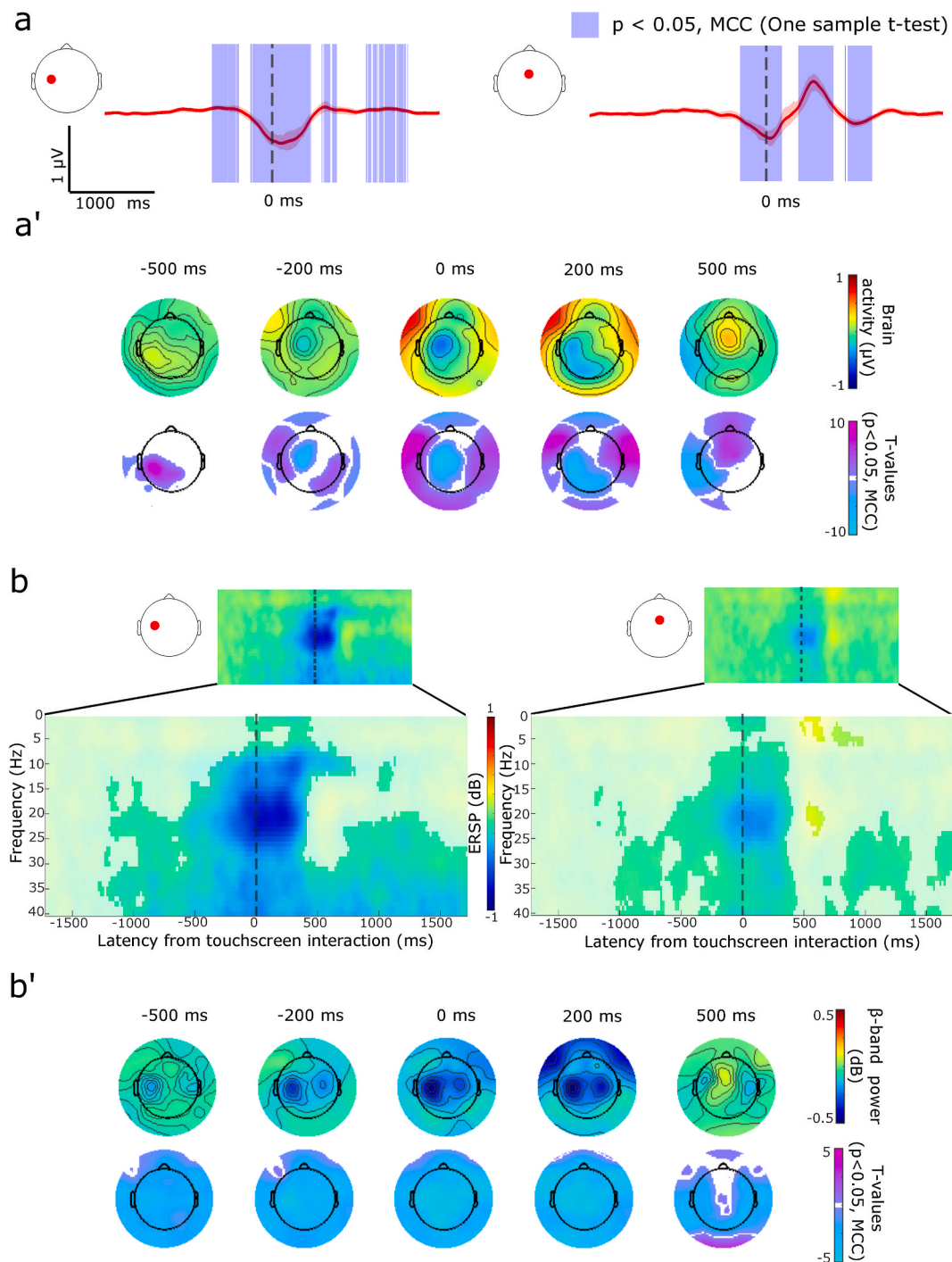


Fig. 1. Event-related potential (participants $N = 66$) and spectral analysis (participants $N = 59$) of EEG signals surrounding smartphone touchscreen interactions. Participants used their right thumb to interact with their smartphone on commonly used apps determined based on usage history. **(a)** Touchscreen interactions show negative deviations at electrodes over the left sensorimotor cortex (left plot, red dot), shown with trimmed means (20%) and 95% confidence intervals. Similar negative deflections occur at a mid-frontal electrode. The data were band-pass filtered between 0.5 and 3 Hz for visualization. Significant statistical clusters were determined by using one-sample t -tests and multiple comparison corrections across all electrodes and time points (MCC, $p < 0.05$, shaded purple in the plot). **(a')** Scalp topologies of trimmed mean signals and T-values show marginal significant positive activity preceding the touchscreen interaction followed by prominent negativity over the sensorimotor cortex. Positive activity recorded over the central to frontal areas occurs after the interaction (MCC, $p < 0.05$). **(b)** Prominent event-related spectral desynchronization was observed over the left sensorimotor cortex (left plot, red dot). A similar pattern was observed over mid-frontal electrodes. **(b')** Scalp topology shows widespread beta-band desynchronization (for visualization, the data is collapsed across the beta-band by estimating the 20% trimmed means at each time point and the significant masked T-values were collapsed by using the maximum absolute amplitude). Significant statistical clusters were determined by using one-sample t -tests and multiple comparison correction (MCC, $p < 0.05$). Approximate times are used for scalp topologies as time information was adjusted due to continuous wavelet transform. For the full statistical outcomes of touchscreen event-related potentials see [Supplementary Movie 1](#), and [Supplementary Movie 3](#) for the event-related spectral potentials (one-sample t -test, focused on the beta-band, touchscreen interactions), and [Supplementary Movie 4](#) (one-sample t -test, focused on the alpha-band). See [Supplementary Movie 2](#) for event-related potentials surrounding touches on a smartphone-like surface. (For interpretation of the references to colour in this figure legend, the reader is referred to the Web version of this article.)

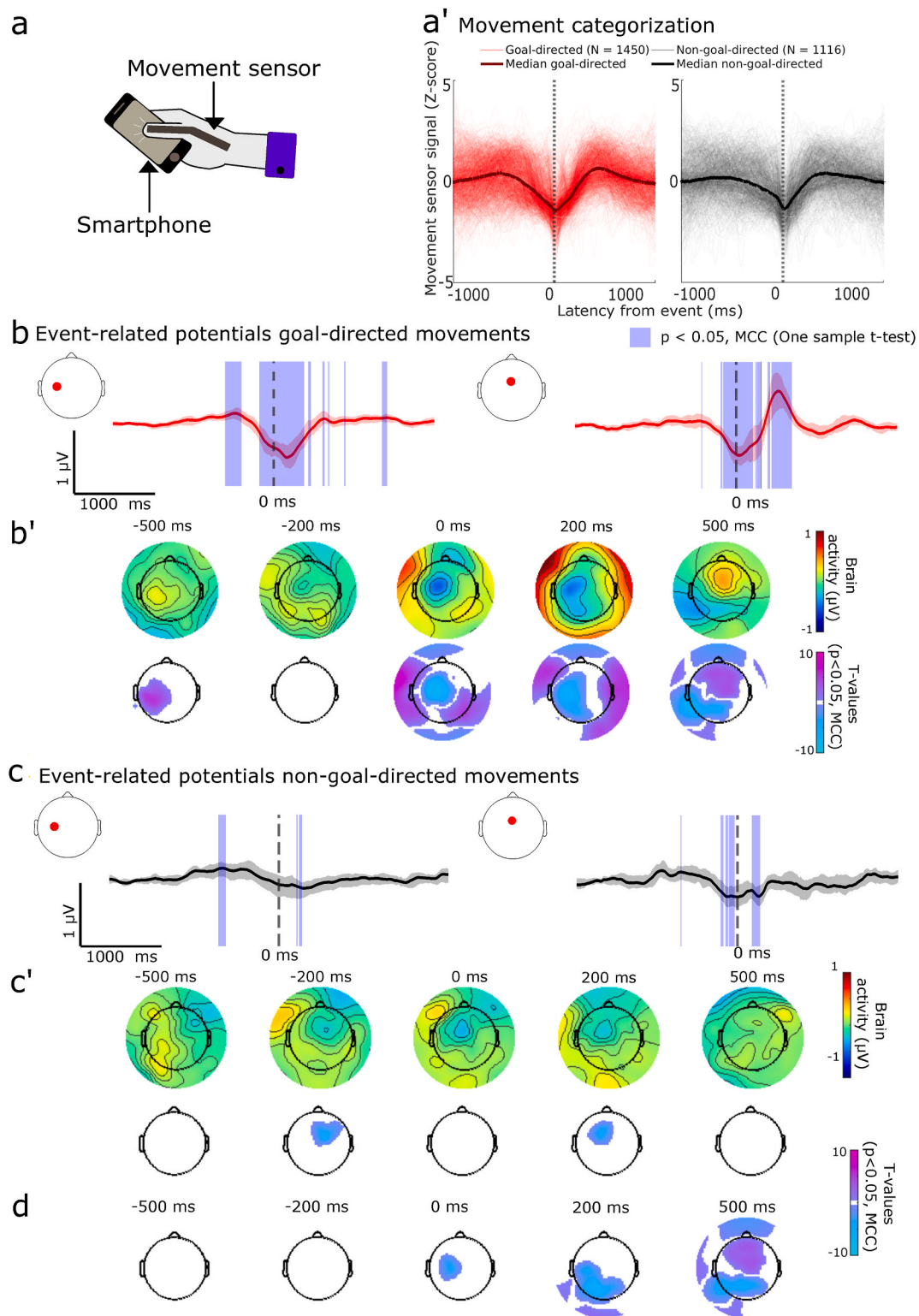


Fig. 2. Movement dynamics and event-related potentials of the goal and non-goal-directed movements (participants N = 32). **(a)** Illustration of the experimental setup. **(a')** Movement signal traces for goal (red, left) and non-goal-directed (black, right) movements time-locked to the predicted events for one participant illustrating the high similarity between the movements (median traces overlaid). Movement signals were Z-score normalized for visualization. **(b-b')** Event-related potential surrounding goal-directed movements show similar activations as touchscreen interactions (one-sample *t*-tests, MCC, $p < 0.05$). Same legend as for main Fig. 1 a-a'. **(c-c')** Event-related potential surrounding non-goal-directed movements show small constrained significant deviations over the left sensorimotor cortex and the midline frontal electrode before and after movement onset. Topological plots show statistically significant clusters on the frontal-to-central electrodes unique to the goal-directed movements. **(d)** Paired samples *t*-tests for goal and non-goal-directed movements for event-related analysis. Significant differences between movements occurred mostly after time-locked events, shown with scalp topographies of T-values after multiple comparison corrections (MCC, $p < 0.05$). For the full statistical outcomes of event-related potentials see [Supplementary Movie 5](#) (one-sample *t*-test goal-directed movement), [Supplementary Movie 6](#) (one-sample *t*-test non-goal-directed movement), and [Supplementary Movie 7](#) (paired *t*-test goal vs. non-goal-directed movements). For p-values of the displayed clusters see [Supplementary Fig. 6](#). (For interpretation of the references to colour in this figure legend, the reader is referred to the Web version of this article.)

directed movements enabling a fair comparison between the neural activations surrounding the two movement types. Unsurprisingly, the patterns for the goal-directed movements were highly similar to the patterns seen for the touchscreen interactions as described above (Fig. 1). Interestingly, there were some notable differences in the event-related potentials between the two movement types.

With regards to the initial sensorimotor signal features, both movement types displayed a slow rising positivity over the contralateral electrodes before the temporal landmarks. However, the subsequent negativity was substantially dampened for the non-goal-directed movements, as they failed to yield statistically significant clusters over the contralateral electrodes (Fig. 2, for full results, see [Supplementary Movie 5](#) – goal-directed movements, [Supplementary Movie 6](#) – for non-goal-directed movements, for paired *t*-test, see [Supplementary Movie 7](#), for model output distributions underlying these analysis see [Supplementary Fig. 3](#)). Interestingly, we discovered a statistically significant cluster corresponding to a negative signal over the ipsilateral sensorimotor cortex before the temporal landmark of the non-goal-directed movements (See between -200 ms and -50 ms, in [Supplementary Movie 6](#), see Fig. 2 for snapshot). The differences between the movements were even more striking after the temporal landmarks. While the goal-directed movements displayed a rich array of activations spanning various regions, there was only a constrained cluster detected over the frontal electrodes for the non-goal-directed movements. The negativity over the fronto-central electrodes was unique to the non-goal-directed movements (and persisted between ~ 200 and 280 ms).

2.4. Desynchronization surrounding the goal-directed movements is dampened for the non-goal-directed movements

We next analyzed the oscillatory hallmarks well implicated in the cortical control of movements. Time locking to the model predicted temporal landmarks confirmed a striking desynchronization (suppressed power) of the alpha, beta, and gamma oscillations for the goal-directed movements, which was similarly observed surrounding the smartphone interactions (Fig. 3, [Supplementary Fig. 4](#), alpha - [Supplementary Movie 8](#), beta - [Supplementary Movie 9](#), gamma - [Supplementary Movie 10](#)). Only a marginal desynchronization of the beta oscillations was observed in the case of non-goal-directed movements predominantly over the contralateral sensorimotor areas (Fig. 3, [Supplementary Movie 11](#)). This desynchronization was temporally constrained between ~ 350 ms preceding the movement to ~ 450 ms after the event. The gamma and alpha oscillations showed similar desynchronizations, but with the gamma signal being more prolonged for the non-goal-directed movements (for topology see [Supplementary Fig. 4](#), gamma - [Supplementary Movie 12](#), alpha - [Supplementary Movie 13](#)). A paired *t*-test established that the non-goal-directed beta desynchronization was marginal in contrast to the goal-directed movements, and revealed statistically significant clusters mostly over the contralateral hemisphere spanning ~ 100 ms before the event to ~ 400 ms after the event ([Supplementary Movie 14](#)).

2.5. Sensorimotor cortical response to tactile stimulation during non-goal-directed movements

The dampened cortical signals during non-goal-directed movements, in contrast to the prominent cortical signals observed during the goal-directed movements, raise the possibility that sensorimotor cortical information processing of sensory inputs from the thumb is suppressed during the non-goal-directed movements. Alternatively, the dampening may be specific to movements and the cortex may continue to process sensory inputs from the hand. To test these ideas, we analyzed the voltage signals stemming from artificial tactile stimulations to the thumb tip coinciding with goal-directed movements (occurring within ± 500 ms) in contrast to those stimulations coinciding with non-goal-directed movements. Notably, the tactile stimulations resulted in strong event-related signals in both conditions over the contralateral

sensorimotor cortex (Fig. 4, goal-directed artificial touches - [Supplementary Movie 15](#), non-goal-directed artificial touches - [Supplementary Movie 16](#)). In sum, although signals are dampened during non-goal-directed movements the sensorimotor cortex remained available for tactile information processing.

3. Discussion

Through time-locking the EEG signals to discrete temporal landmarks associated with smartphone behavior we identified a range of neural processes, and some of these processes were unique to smartphone use. Strikingly, when engaged on the smartphone, not all of the generated movements resulted in touchscreen interactions. These non-goal-directed movements were processed differently by the brain as opposed to the goal-directed movements. Our findings provide a comprehensive overview of how the brain engages in smartphone interactions and highlights the importance of studying real-world behaviors to discover novel neural processes.

The neural signals time-locked to the smartphone touchscreen events revealed unique patterns of activity that may not be observed in common laboratory paradigms. First, the events were preceded by a slow build-up of positivity over the contralateral sensorimotor electrodes. In conventional paradigms a similar positivity – albeit over central electrodes and inconsistently observed – correlates with voluntary action inhibition (Misirlisoy and Haggard, 2014; Shibasaki and Kato, 1975). Our findings where this putative inhibitory signature is followed by negativity raise the possibility that motor outputs emerge from a competitive process that requires overcoming underlying neural inhibition (Duque et al., 2017). Second, motor preparation of the conventional artificial tasks – from reaction time to instructed voluntary key presses – showed bilateral negativity over the sensorimotor electrodes (and this was confirmed here in a subset of the participants generating smartphone-like voluntary thumb movements upon instruction), whereas only a contralateral (to movement) negativity was found surrounding the smartphone touch (Shibasaki and Hallett, 2006; Urbano et al., 1998). This ipsilateral disengagement for motor control could stem from the day-to-day repetition of smartphone interactions resulting in a highly optimized circuitry negating inter-hemispheric interactions for motor control, or may reflect top-down processes that suppress ipsilateral activity to promote motor learning (Lacourse et al., 2005; Kobayashi et al., 2009). Either way, the ipsilateral disengagement must be highly context-dependent as, when performing an artificial task, the ipsilateral hemisphere was vividly engaged for the same type of thumb movements.

The touchscreen events did evoke some familiar neural signals associated with visual processing – i.e., bilateral negativity over the occipital electrodes and a subsequent (~ 250 ms after the visual response) frontal-to-central positive wave. While the former probably indicates the visual processing of the new content on the screen triggered by the touch, the latter may indicate subsequent information consolidation involving memory processes (Polich, 2007). According to the time-frequency analysis, the touchscreen events were surrounded by robust beta and alpha-band desynchronizations. These desynchronizations are commonly reported for voluntary movements and indicate increased excitability in the populations engaged in movement-related sensorimotor processing (Neuper and Pfurtscheller, 2001). A rebound of beta-oscillations was observed at ~ 500 ms after the touchscreen event, which may reflect an inhibited motor cortical state and signal action completion to other brain areas (Heinrichs-Graham et al., 2017).

Our findings suggest that much of the neural processing during smartphone behavior is dedicated to non-goal-directed movements, and such movements have been long ignored as conventional tasks fixate on highly instructed movements. Still, the familiar signal features – based on artificial tasks – provided some hints on the neural underpinnings of these apparently unnecessary movements. The movements were associated with a rising positivity over the contralateral sensorimotor

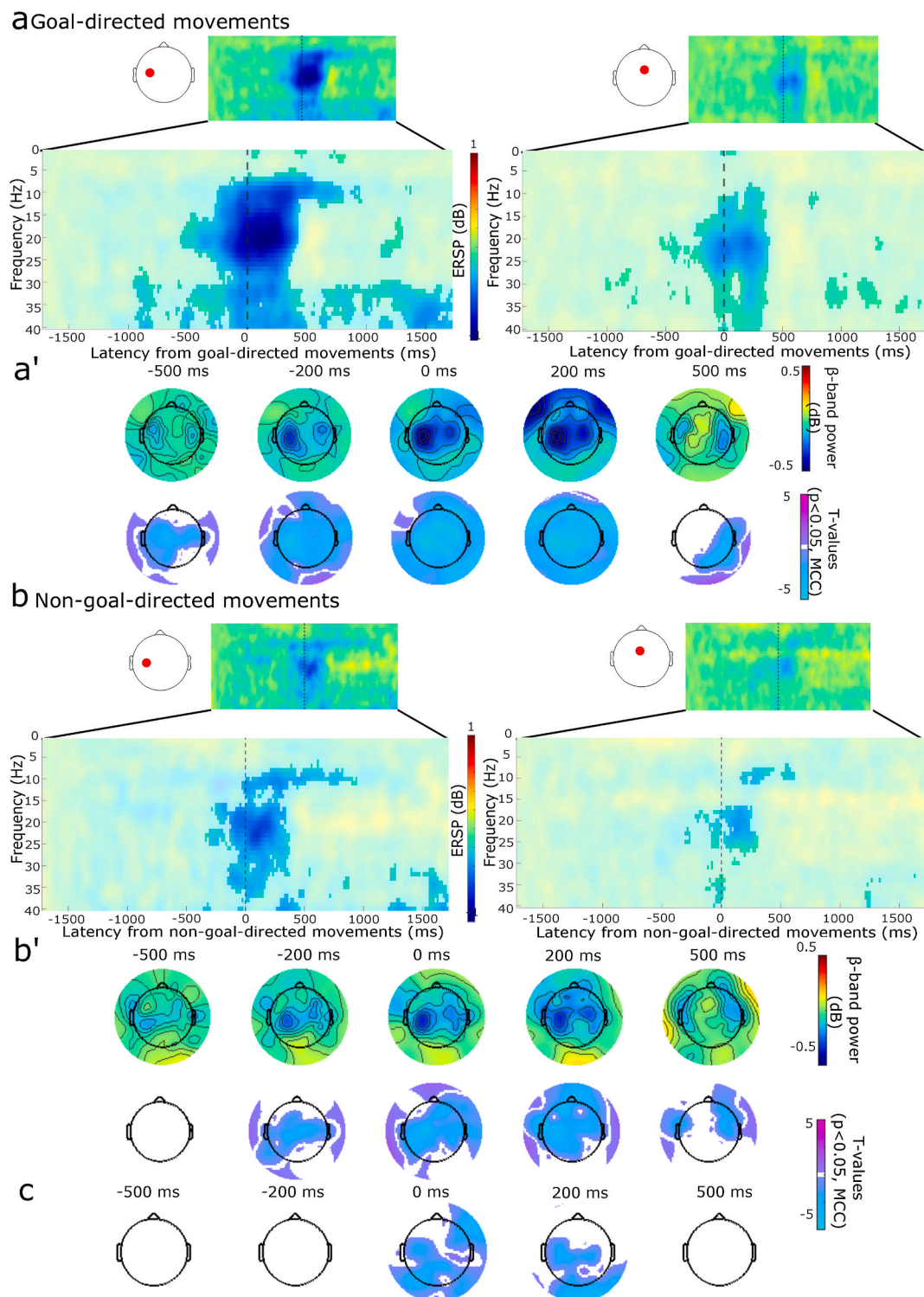


Fig. 3. Event-related spectral analysis for goal and non-goal-directed movements (participants $N = 29$). **(a-a')** Goal-directed movements. Desynchronization was recorded over the left sensorimotor cortex and mid-frontal electrodes. Same legend as in Fig. 1b-b'. **(b)** Surrounding non-goal-directed movements, highly constrained beta and gamma-band desynchronization were recorded at the electrodes over the left sensorimotor cortex and midline frontal areas. **(b')** The beta-band desynchronization was spatially and temporally constrained. **(c)** Paired samples t -tests for goal and non-goal-directed movements for event-related spectral analysis. Statistically, significant clusters show different event-related spectral desynchronization between the movements in the beta-band. Approximate times were used for scalp topographies as time information was adjusted due to continuous wavelet transform. For alpha-band topologies see Supplementary Fig. 4. For full statistical outcomes of the event-related spectral analysis see Supplementary Movie 8 (one-sample t -test, alpha-band, goal-directed movements), Supplementary Movie 9 (one-sample t -test, beta-band, goal-directed movements), Supplementary Movie 10 (one-sample t -test, gamma-band, goal-directed movements), Supplementary Movie 11 (one-sample t -test, beta-band, non-goal-directed movements), Supplementary Movie 12 (one-sample t -test, gamma-band, non-goal-directed movements), Supplementary Movie 13 (one-sample t -test, alpha-band, non-goal-directed movements), Supplementary Movie 14 (paired t -test goal vs. non-goal-directed movements). For p -values of the displayed clusters see Supplementary Fig. 7.

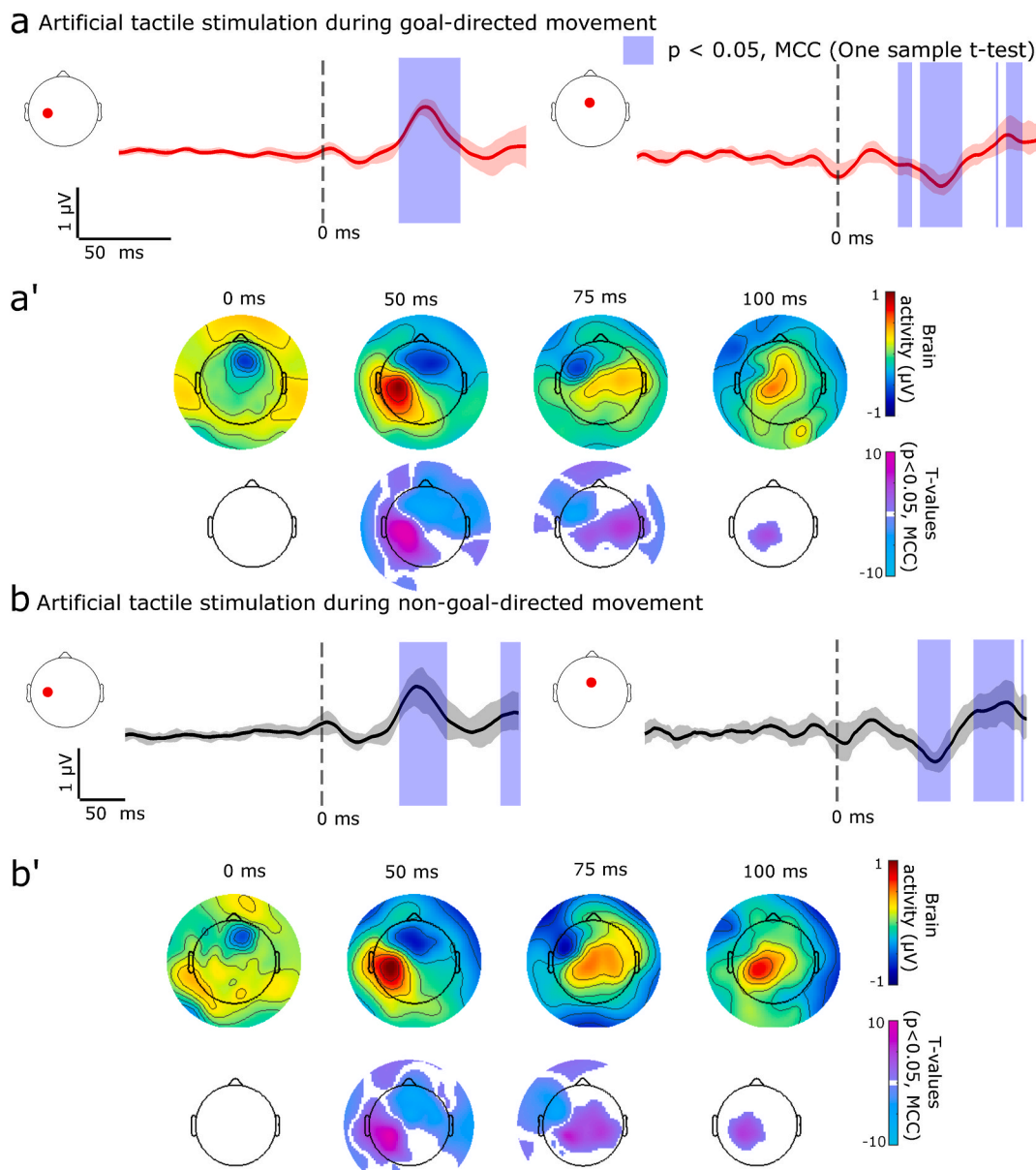


Fig. 4. Event-related potentials for artificial tactile stimulations coinciding with the goal (participants $N = 29$) and non-goal-directed (participants $N = 22$) movements. **(a)** Statistically significant clusters (denoted with purple overlay) involving a positive component were observed after the artificial tactile stimulation during goal-directed movement over the left sensorimotor cortex (left plot, red dot). A negative component was observed at the mid-frontal electrode. **(a')** Scalp topologies show statistically significant clusters over the sensorimotor cortex. **(b-b')** A near-identical pattern of signals was visible when the stimulations coincided with the non-goal-directed movement. Significant statistical clusters were identified using one-sample t -tests and multiple comparisons corrected (MCC, $p < 0.05$). For full statistical outcomes see [Supplementary Movie 15](#) (one-sample t -test, goal-directed movements coinciding with artificial touches), [Supplementary Movie 16](#) (one-sample t -test, non-goal-directed movements coinciding with artificial touches). (For interpretation of the references to colour in this figure legend, the reader is referred to the Web version of this article.)

electrodes – suggesting that the speculative action inhibition processes must be overcome for non-goal-directed movements as well. The subsequent negativity over the contralateral sensorimotor electrodes, and the beta-band desynchronization, were substantially diminished for the non-goal-directed movements compared to the goal-directed movements. These findings on the beta-band oscillations are akin to the correlates of non-goal-directed eye movements recently captured in non-human primates and humans aimlessly performing finger movements (Sendhilnathan et al., 2021; Pereira et al., 2017). As suggested in non-human primates based on invasive neural recordings, these diminished signals may either stem from greater trial-to-trial neural variability or due to more limited recruitment of neural populations (Sendhilnathan et al., 2021). We found a negative signal over the

ipsilateral sensorimotor electrodes for the non-goal-directed movements. Perhaps these activations are related to inter-hemispheric interactions needed to absorb the broad consequences of the non-goal-directed movements.

The diminished motor signals surrounding the non-goal-directed movements may stem from a general dampening or gating of sensorimotor processing. We used artificial tactile stimulation to probe if the sensorimotor cortex remained similarly responsive during the non-goal-directed movements as during the goal-directed movements. Similar amplitudes of early cortical signals were observed for the artificial tactile inputs irrespective of them coinciding with goal vs. non-goal-directed movements. While this does provide evidence for the cortex remaining responsive to inputs from the thumb even during the non-

goal-directed movements, the similar amplitudes do not necessarily mean that the artificial signals were identically processed in the two conditions, as the tactile stimulations occurred in distinct sensory contexts. In the goal-directed condition the artificial stimulations were interspersed with the real tactile feedback whereas the feedback was absent for the non-goal-directed movements.

The activation at the visual electrodes and the consolidation-oriented signals were absent for the non-goal-directed movements. It remains unclear if the brain pre-emptively the inconsequential nature of the non-goal-directed movements at the time of motor preparation to suppress visual processing, or if the absent visual processing can be explained by the lack of a trigger in the form of a tactile event or visual content change. The brain may even keep track of the outcomes of the non-goal-directed movements, and signal these erroneous occurrences to the downstream processes to impact visual processing. Indeed, we discovered frontal negativity (mimicking the error-related negativity) following the non-goal-directed movements but this was not observed for the goal-directed movements (van Schie et al., 2004; Riesel, 2019).

Our study had some notable limitations. First, our methodological framework – which included aligning different hardware clocks in a data-driven manner – resulted in the rejection of several participants. While these rejections ensured aligned signals and enabled a comparison of kinematically similar movements with distinct outcomes (i.e. goal vs. non-goal-directed), they do warrant methodological improvements to minimize the rejections. Second, we used the event-related potential analytical framework and the signals were baseline corrected using a pre-event period. We cannot rule out that the neural signals of the surrounding events impacted our analysis via the baseline correction. Indeed, conventional ERP analysis recommend an inter-trial period of ~10 s when studying movements (Pfurtscheller and Lopes da Silva, 1999). However, spontaneous smartphone interactions are dominated by shorter inter-touch intervals and this required us to sidestep the conventional recommendation (Pfister and Ghosh, 2020). Still, as in this study the movements occurred in a mixed order, any impact of the short intervals on the baseline correction was likely shared by both the goal and the non-goal directed neural signals, driving our notion that the comparison between the two signals remains interpretable. Further supporting the analysis, the preceding behavioral intervals were substantially jittered attenuating any rapid neural signals in the baseline period, and if any slow signals were triggered by the preceding event they were likely diminished using the applied high pass (>0.5 Hz). Indeed, the neural signals following the baseline period did not significantly deviate from 0 till ~700 ms prior to the behavioral event (or ~800 ms after the baseline period). Future research could explicitly attempt to unmix the influence of neighboring behavioral events on the baseline (if any) by using signal deconvolution (Lütkenhöner, 2010). Third, as our analysis was focused on the kinematically similar movements, the neural correlates of those movements which did not simply meet the conditions of our binary categories remained unexplored. Fourth, we established the movement profiles using a movement sensor attached to the right thumb. More information (say using additional visual recordings) on the movements could improve the analysis by informing on the gestures used. Related to this, the sensor was oblivious to the complex postural dynamics ultimately resulting in different distances between the starting position of the thumb on the screen. Here, we circumvented this variance by studying normalized signals but by using additional sensors these dynamics and their neural correlates could be established. The instruction to use the right thumb may have also disturbed the natural smartphone use posture. Finally, as a notable limitation, our assumption that the movements that do not result in a touch are non-goal-directed is open to challenge. While they seem erroneous based on the error-related negativity signal, more data on the movements and subjective self-reports (Schultze-Kraft et al., 2016) may be leveraged in the future to further confirm or refute this assumption.

Despite the limitations, this study demonstrates a fresh approach to study neural processes in the real world. Unlike conventional cognitive

tasks – focused on specific cognitive processes – a range of neural processes are measurable surrounding the smartphone interactions. Future research can help parse the neural networks engaged in this ubiquitous behavior. Extending our approach with longer recordings periods – yielding a larger number of events – may also be leveraged to address the differences in neural activity from one smartphone event to the next. Indeed, our results indicate that distinct neural processes underlie the behavioral events classified as goal vs. non-goal-directed movements. Still, why the non-goal-directed movements occur at all is not clear. These movements may be a by-product of the cortical-sub-cortical interactions. For instance, subcortical structures may help prepare multiple actions in parallel, and some of these may be released as non-goal-directed movements (Cisek and Kalaska, 2010). Furthermore, the role of the cortex in these movements is also not clear. The dampened signals could stem from the engagement of deep, scattered, or highly variable neural signal sources. Resolving the sources of the non-goal-directed movements offers exciting avenues for future research. For instance, using resolved sources we can address if the different movements involve overlapping neural populations or if these distinct movements originate from distinct neural computations. Furthermore, it would become possible to address how the motor and sensory areas orchestrate such that the non-goal-directed movements do not interfere with processing the smartphone information. The neural signals time-locked to the smartphone events in themselves provide a new and highly accessible way to study how various neural processes combine to enable real-world behavior. We anticipate this will enable real-world focused research well beyond fundamental cognitive science, for instance to discover markers of neurological dysfunctions based on the *smartphone related potentials* described here. In conclusion, a combination of data-driven behavioral models in conjunction with neural recordings, and prior research using event-related potentials, make the complex neural signals time locked to real-world behavioral events interpretable and possibly broadly useful.

4. Methods

4.1. Participants

Healthy right-handed volunteers (self-declared) were recruited by using on-campus advertisements for a large study deploying multiple sensors to improve the fundamental understanding of smartphone behavior. From this recruitment drive, 106 subjects participated in measurements containing the sensor data required for this study (56 females) from 18 to 46 (median age of 24). All participants provided written and informed consent, and the study was approved by the Institute of Psychology Ethics Committee at Leiden University. For an overview of participants and the different stages of participant elimination due to technical limitations see Supplementary Methods.

4.2. Instructed movements on a smartphone-like box

To capture the common movement-related EEG signals associated with artificial tasks, we instructed participants (twenty-seven of the recruited subjects) to touch a dummy smartphone-like box, attached to a force sensor (Interlink Electronics, Camarillo). They were instructed to touch a target on the box whenever they felt like within 5 s (with a 5-s clock visible to the user). The force sensor signals captured the interactions. The touches on the force sensor did not yield any digital feedback, and only touches that occurred within the 2 mm target perimeter were recorded. The force sensor output was gathered using a USB 6008 DAQ (National Instruments, Austin).

4.3. Smartphone data collection

Participants installed the TapCounter app (QuantActions AG, Zurich) before the laboratory visit. The app operated in the background and

gathered the timestamps of each interaction with a millisecond resolution, and with a typical error of 0 ms (Balerna and Ghosh, 2018). Participants were instructed to use the two most used social and two non-social apps, based on their behavior gathered before the laboratory measure (Balerna and Ghosh, 2018) (See Supplementary Methods for an overview of the apps used according to the frequency of goal and non-goal-directed movements). Participants were instructed to only use their right thumb during the laboratory measure and this was further verified online by using video recordings (For an illustrative video of the experimental setup see [Supplementary Movie 17](#)). The usage sessions lasted for ~1 h and participants were encouraged to take short (<1 min) breaks every 10 min.

4.4. Artificial tactile stimulation

Compact solenoid tactile stimulators (Tactor, Dancer Design, Merseyside) were attached to the thumb tip by using double-sided stickers and further wrapped with a conductor such that participants could freely interact with the capacitive smartphone touchscreen. The solenoid was activated by using square wave pulses (10 ms) spaced by a uniform distribution of intervals spanning 0.75 s – 1 s. A copy of the stimulation trigger (TTL) was registered by the EEG equipment. The thumb was further covered with a conductive surface (common aluminum foil) ensuring that all the touches were translated to touchscreen events and that the same part of the thumb was used to target the screen.

4.5. Movement sensor recordings

The right thumb flexions were tracked using a movement sensor (Flex Sensor, 112 mm, Digi-Key, Thief River Falls). The sensor was attached to the thumb (dorsum) using a custom-built jacket that allowed the sensor to bend within the jacket without the sensor being pulled. The analog signals from the sensor were digitized at 1 kHz using Labview via the USB 6008 DAQ (National Instruments, Austin, USA). The same DAQ was also used to power the sensor. The thumb was able to freely move on the touchscreen under this configuration. As the EEG and the movement sensors operated on different clocks, they were synchronized using common TTL pulse bursts generated by using an IBM T 42 computer running MATLAB. The movement signals were bandpass filtered in the range of 1–10 Hz (for an example of the recorded kinematic signals see Supplementary Methods).

4.6. Alignment of smartphone data to the common laboratory clock

We formulated a data-driven method to align the smartphone data – recorded using the smartphone operating system (Android) clock – to the common laboratory clock (used for EEG, force sensor and movement-sensor recordings). As TTL pulses could not be injected into the smartphone (without software adjustments), we trained a model to link the movement sensor signal to the force sensor signals. The model was a global bidirectional LSTM (BI-LSTM) regression model that used movement sensor values and 100 extracted moving averages values (equally weighted, calculated over a sliding window of 10 ms) as inputs (Graves and Schmidhuber, 2005). The model predicted the force of touch, we inferred that the high model predicted force emulated a touchscreen interaction. Mean squared error was chosen as the model cost function. The architecture consisted of 2 BI-LSTM layers followed by a fully connected layer. Before training the model, each participant's data was split into the train (80%), validation (10%), and test (10%) sets. The model was trained in batches of 10 (z-score normalized) samples obtained by randomly selecting sequences of length 1000 ms. Following the training, we obtained a mean squared error (capturing the difference between real force vs. predicted force) of 0.1120 on the test set, 0.1097 on the train set, and 0.0877 on the validation set. The alignment was performed by correcting for the delay between the

touchscreen interactions and the model-predicted force. As the model relied on movement sensor signal fluctuations, subjects without systematic movement sensor signals surrounding the smartphone touches, and subjects where the signals appeared misaligned were eliminated resulting in 68 participants for further consideration (see Supplementary Methods).

4.7. Identification of goal and non-goal-directed movements

After the technical alignment, we identified goal and non-goal-directed movements based on the outputs of a (separate from the one used for alignment) artificial neural network (ANN) trained to identify smartphone interactions using kinematic inputs. This involved two methodological steps. First, at the level of each individual a classification ANN was trained with touchscreen interactions and z-score normalized approximate integrals extracted from processed movement sensor signals. To decrease class imbalance, touchscreen interactions were padded with ± 30 samples and the datasets were undersampled by a factor of 10 before training. Second, the model predictions were contrasted against the real outputs and non-goal-directed movements were identified based on a predicted interaction that did not coincide with a real touchscreen interaction (false-positive errors, [Supplementary Fig. 1a-a'](#)).

The ANN model contained a 1-D Convolutional layer with 100 kernels for automatic feature extraction. Followed by three BI-LSTM layers. Three Dropout layers, with a dropout rate of 0.5, were applied in between each BI-LSTM layer to prevent overfitting. Finally, a fully connected layer with sigmoid activation was used for the classification. Binary cross entropy was chosen as the model cost function. The ANNs were trained in batches of 10 samples obtained by randomly selecting sequences of length 200 ms. After undersampling of the data, a sequence of length 200 represented 2 s of the raw data. Considering that the movement generally occurred within a duration of 2 s ([Supplementary Fig. 2](#)), the chosen sequence length was enough to capture a movement. For one pass of the training dataset (epoch), the number of generated batches was calculated as the total length of the train data divided by 200 ms. A maximum of 100 epochs was set for training. However, the ANNs were stopped after 30 epochs with no improvement in the number of true positive predictions in the validation set. Furthermore, the learning rate was adjusted by a factor of 0.1 after no improvement for 5 epochs on the number of true positives in the validation set. For the validation set, no shuffling or random sampling was used, essentially keeping the validation data across epochs the same allowing for a direct comparison between the number of true positives in the validation set. For the final evaluation, we used the F2 score due to its higher emphasis on recall as opposed to precision (see Supplementary Methods for model hyperparameters).

After training, goal and non-goal-directed movements were identified based on the model predictions. The ANN made continuous predictions of the probability of a class label, a value between 0 and 1. The final predictions of each model were selected by comparing each output probability to a threshold (between 0 and 1) and by assigning class 1 when the value was above the selected threshold and class 0 otherwise. The F2 score was calculated for every possible threshold and the threshold that yielded the highest F2 score was selected. For each participant, the model predictions above the threshold with the highest F2 score were used to identify the goal and non-goal-directed movements. The ANN was trained with a window of touchscreen interactions. Consequently, the predicted peaks were expected approximately around (and not exactly at) the interaction. Any predicted peak around ± 100 ms of the touchscreen interaction was considered a correct prediction (goal-directed movement). The value of ± 100 ms was selected based on the peak width of the model predictions averaged across all participants ([Supplementary Fig. 3](#)). Finally, a non-goal-directed movement was identified with a model prediction where there was no touchscreen interaction in the vicinity (false-positive errors). This was defined as any

peak of a model prediction further than ± 1 s from the interaction, based on the typical movement completion durations. The predictions ranging from 100 ms to 1 s were ignored.

4.8. EEG data collection and pre-processing

EEG data were collected while subjects were comfortably seated in a Faraday cage. Sixty-four channel EEG caps with equidistant electrodes were used (EasyCap GmbH, Wörthsee, Germany) in conjunction with ABRALYT HiCl electrode gel. The data was gathered using the 64-channel DC amplifier BrainAmp (Brain Products GmbH, Gilching). The signals were recorded and digitized at 1 kHz. All of the EEG data processing was performed offline using EEGLAB running on MATLAB (MathWorks, Natick) (Delorme and Makeig, 2004). All channels with impedances higher than 10 k Ω were removed and then subsequently replaced by interpolation. Furthermore, we used Independent Component Analysis (Infomax, called using pop_runica implemented in EEGLAB) to remove the blink-related artifacts (Pontifex et al., 2017). Towards the analysis of event-related potentials, the data were bandpass filtered between 0.5 Hz and 30 Hz, and for event-related spectral analysis, the data were bandpass filtered between 0.5 Hz and 45 Hz. The two ocular electrodes placed under the eyes were removed from the statistical analyses.

Towards the event-related analysis surrounding the movements and touchscreen interactions (i.e., time-locked to the goal and non-goal-directed movements), the data was epoched using a -2 s to $+2$ s window surrounding the event, and the period between -2 s and -1.5 s was used as a baseline. We chose this baseline period to study the motor preparatory activity that is anticipated to begin at ~ 1.5 s prior to the movement (Jankelowitz and Colebatch, 2002). Trials crossing ± 80 μ V were rejected as measurement artifacts. Further statistical analysis was performed on participants with greater than 50 remaining trials per movement type. Towards the analysis surrounding the artificial touches (where a solenoid was used to deliver an artificial touch see above), the data was epoched using a -100 ms window surrounding the event, and the period between -100 ms and -25 ms was used as the baseline (to contrast against pre-stimulus activity). The data was bandpass filtered between 1 Hz and 45 Hz. The spectrograms were estimated at each electrode using continuous wavelet transform (Frequencies 1–40 Hz, Morlet wavelet, 1 cycle-wavelet expanding to 70%).

4.9. Statistical analysis

The event-related signals were analyzed using one-sample and paired *t*-tests (goal vs. non-goal-directed movements) across all electrodes and time points (and frequency range of 1–40 Hz) using the mass univariate linear modeling toolbox LIMO EEG (Pernet et al., 2011). Towards follow-up analysis, the same toolbox was used at the level of each individual – with movement categories and neural network model predicted peaks as a covariate – to obtain ANCOVA outputs. These outputs were then used toward population-level one-sample *t*-tests. In this follow-up applied to the frequency analysis, for computational efficiency, only the beta-band was considered (12–30 Hz). The statistics were based on trimmed means (20 percent). The time range considered for statistical analysis was identical to the epoching windows. The statistics were corrected for multiple comparisons by using spatiotemporal clustering as implemented in LIMO EEG ($\alpha = 0.05$, 1000 bootstraps).

Author contributions

A.G. conceived the study. A.G., R.K. and E.C. designed the study. R.K. analyzed the data aided by E.C. and A.G.. A.G. drafted the report aided by L.G. and R.K. All authors helped edit the manuscript.

Code availability

Codes used for processing the kinematic and EEG signals including

the model settings are shared via GitHub (https://github.com/CODELABLEIDEN/Non_goal_directed_smartphone_2022).

Funding

This study was funded by a research grant from Velux Stiftung (no. 1283, A.G. is principal investigator) and Brain@home (no. 114025101, A.G. as co-investigator) which is co-funded by Health-Holland, Top Sector Life Sciences & Health, and ZonMw. This research was also supported by the SNSF Early Postdoc.Mobility (no. 199692, awarded to E.C. with A.G. as host).

Declaration of competing interest

The authors declare the following financial interests/personal relationships which may be considered as potential competing interests: A. G. is a co-founder of QuantActions AG., Zurich, Switzerland, and E.C. is a founding team member. This company focuses on converting smartphone taps to mental health indicators. Software and data collection services from QuantActions were used to monitor smartphone activity. A.G. has a filled patent related to the data alignment tools used here. Authors R.K. and L.G. have no competing interests to report.

Data availability

The data is available on dataverse.nl within a month following the publication.

Acknowledgment

The authors would like to thank the student assistants who contributed to the data collection at Leiden University. The authors appreciate the discussions with Dr. Arnoud Visser at the University of Amsterdam and the feedback from Sebo Uithol and Gerd Tinkenhauser. We thank Evert Dekker for his assistance in developing the movement sensors used in this study.

Appendix A. Supplementary data

Supplementary data to this article can be found online at <https://doi.org/10.1016/j.yrnip.2023.100164>.

References

- Adams, M.S., Popovich, C., Staines, W.R., 2017. Gating at early cortical processing stages is associated with changes in behavioural performance on a sensory conflict task. *Behav. Brain Res.* 317, 179–187.
- Balerna, M., Ghosh, A., 2018. The details of past actions on a smartphone touchscreen are reflected by intrinsic sensorimotor dynamics. *Npj Digit. Med.* 1, 4.
- Cisek, P., Kalaska, J.F., 2010. Neural mechanisms for interacting with a world full of action choices. *Annu. Rev. Neurosci.* 33, 269–298.
- Delorme, A., Makeig, S., 2004. EEGLAB: an open source toolbox for analysis of single-trial EEG dynamics including independent component analysis. *J. Neurosci. Methods* 134, 9–21.
- Duque, J., Greenhouse, I., Labruna, L., Ivry, R.B., 2017. Physiological markers of motor inhibition during human behavior. *Trends Neurosci.* 40, 219–236.
- Graves, A., Schmidhuber, J., 2005. Framework phoneme classification with bidirectional LSTM and other neural network architectures. *Neural Network.* 18, 602–610.
- Heinrichs-Graham, E., Kurz, M.J., Gehringer, J.E., Wilson, T.W., 2017. The functional role of post-movement beta oscillations in motor termination. *Brain Struct. Funct.* 222, 3075–3086.
- Houdayer, E., Lee, S.-J., Hallett, M., 2020. Cerebral preparation of spontaneous movements: an EEG study. *Clin. Neurophysiol.* 131, 2561–2565.
- Ingram, J.N., Kording, K.P., Howard, I.S., Wolpert, D.M., 2008. The statistics of natural hand movements. *Exp. Brain Res.* 188, 223–236.
- Ingram, J.N., Wolpert, D.M., 2011. In: Green, A.M., Chapman, C.E., Kalaska, J.F., Lepore, F. (Eds.), Chapter 1 - Naturalistic Approaches to Sensorimotor Control” in *Progress In Brain Research, Enhancing Performance for Action and Perception*. Elsevier, pp. 3–29.
- Jankelowitz, S., Colebatch, J., 2002. Movement-related potentials associated with self-paced, cued and imagined arm movements. *Exp. Brain Res.* 147, 98–107.

- Kayser, C., Kording, K.P., Konig, P., 2004. Processing of complex stimuli and natural scenes in the visual cortex. *Curr. Opin. Neurobiol.* 14, 468–473.
- Kilavik, B.E., Zaepffel, M., Brovelli, A., MacKay, W.A., Riehle, A., 2013. The ups and downs of beta oscillations in sensorimotor cortex. *Exp. Neurol.* 245, 15–26.
- Kobayashi, M., Theoret, H., Pascual-Leone, A., 2009. Suppression of ipsilateral motor cortex facilitates motor skill learning. *Eur. J. Neurosci.* 29, 833–836.
- Kristeva, R., Cheyne, D., Lang, W., Lindinger, G., Deecke, L., 1990. Movement-related potentials accompanying unilateral and bilateral finger movements with different inertial loads. *Electroencephalogr. Clin. Neurophysiol.* 75, 410–418.
- Lacourse, M.G., Orr, E.L.R., Cramer, S.C., Cohen, M.J., 2005. Brain activation during execution and motor imagery of novel and skilled sequential hand movements. *Neuroimage* 27, 505–519.
- Leocani, L., Toro, C., Zhuang, P., Gerloff, C., Hallett, M., 2001. Event-related desynchronization in reaction time paradigms: a comparison with event-related potentials and corticospinal excitability. *Clin. Neurophysiol.* 112, 923–930.
- Lutkenhoner, B., 2010. Baseline correction of overlapping event-related responses using a linear deconvolution technique. *Neuroimage* 52, 86–96.
- Matsumoto, K., Tanaka, K., 2004. The role of the medial prefrontal cortex in achieving goals. *Curr. Opin. Neurobiol.* 14, 178–185.
- Mehrabian, A., Friedman, S.L., 1986. An analysis of fidgeting and associated individual differences. *J. Pers.* 54, 406–429.
- Misirlisoy, E., Haggard, P., 2014. Veto and Vacillation: a neural precursor of the decision to withhold action. *J. Cognit. Neurosci.* 26, 296–304.
- Neuper, C., Pfurtscheller, G., 2001. Event-related dynamics of cortical rhythms: frequency-specific features and functional correlates. *Int. J. Psychophysiol.* 43, 41–58.
- Pereira, J., Ofner, P., Schwarz, A., Sburlea, A.I., Muller-Putz, G.R., 2017. EEG neural correlates of goal-directed movement intention. *Neuroimage* 149, 129–140.
- Pernet, C.R., Chauveau, N., Gaspar, C., Rousset, G.A., 2011. LIMO EEG: a toolbox for hierarchical Linear Modeling of ElectroEncephaloGraphic data. *Comput. Intell. Neurosci.* 10.1155/2011/831409 (Accessed 25 January 2019).
- Pfister, J.-P., Ghosh, A., 2020. Generalized priority-based model for smartphone screen touches. *Phys. Rev. E* 102, 012307.
- Pfurtscheller, G., Lopes da Silva, F.H., 1999. Event-related EEG/MEG synchronization and desynchronization: basic principles. *Clin. Neurophysiol.* 110, 1842–1857.
- Picton, T.W., 1992. The P300 wave of the human event-related potential. *J. Clin. Neurophysiol.* 9, 456–479.
- Polich, J., 2007. Updating P300: an integrative theory of P3a and P3b. *Clin. Neurophysiol.* 118, 2128–2148.
- Pontifex, M.B., Miskovic, V., Laszlo, S., 2017. Evaluating the efficacy of fully automated approaches for the selection of eyeblink ICA components. *Psychophysiology* 54, 780–791.
- Qing Cui, R., Deecke, L., 1999. High resolution DC-EEG analysis of the Bereitschaftspotential and post movement onset potentials accompanying uni- or bilateral voluntary finger movements. *Brain Topogr.* 11, 233–249.
- Riesel, A., 2019. The erring brain: error-related negativity as an endophenotype for OCD—a review and meta-analysis. *Psychophysiology* 56, e13348.
- Rossini, P.M., et al., 1999. “Gating” of human short-latency somatosensory evoked cortical responses during execution of movement. A high resolution electroencephalography study. *Brain Res.* 843, 161–170.
- Schultze-Kraft, M., et al., 2016. The point of no return in vetoing self-initiated movements. *Proc. Natl. Acad. Sci. USA* 113, 1080–1085.
- Sendhilnathan, N., Basu, D., Goldberg, M.E., Schall, J.D., Murthy, A., 2021. Neural correlates of goal-directed and non-goal-directed movements. *Proc. Natl. Acad. Sci. USA* 118.
- Shibasaki, H., Hallett, M., 2006. What is the Bereitschaftspotential? *Clin. Neurophysiol.* 117, 2341–2356.
- Shibasaki, H., Kato, M., 1975. Movement-associated cortical potentials with unilateral and bilateral simultaneous hand movement. *J. Neurol.* 208, 191–199.
- Sonkusare, S., Breakspear, M., Guo, C., 2019. Naturalistic stimuli in neuroscience: critically acclaimed. *Trends Cognit. Sci.* 23, 699–714.
- Staines, W.R., Brooke, J.D., McIlroy, W.E., 2000. Task-relevant selective modulation of somatosensory afferent paths from the lower limb. *Neuroreport* 11, 1713.
- Urbano, A., Babiloni, C., Onorati, P., Babiloni, F., 1998. Dynamic functional coupling of high resolution EEG potentials related to unilateral internally triggered one-digit movements. *Electroencephalogr. Clin. Neurophysiol.* 106, 477–487.
- van Schie, H.T., Mars, R.B., Coles, M.G.H., Bekkering, H., 2004. Modulation of activity in medial frontal and motor cortices during error observation. *Nat. Neurosci.* 7, 549–554.